ELSEVIER

Journal of Photochemistry and Photobiology A: Chemistry 137 (2000) 53–62

Journal of Photochemistry and Photobiology A:Chemistry

www.elsevier.nl/locate/jphotochem

TiO_2-mediated photodegradation of liquid and solid organic compounds

Toshihiro Minabe [a,*], Donald A. Tryk [a], Phillip Sawunyama [b], Yoshihiko Kikuchi [b], Kazuhito Hashimoto [c], Akira Fujishima [a]

[a] *Department of Applied Chemistry, School of Engineering, The University of Tokyo, 7-3-1 Hongo, Bunkyo-ku, Tokyo 113-8656, Japan*
[b] *Kanagawa Academy of Science and Technology, 1583 Iiyama, Atsugi, Kanagawa 243-0297, Japan*
[c] *Research Center for Advanced Science and Technology, The University of Tokyo, 4-6-1 Komaba, Meguro-ku, Tokyo 153-8904, Japan*

Received 2 March 2000; received in revised form 17 July 2000; accepted 3 August 2000

Abstract

The photocatalytic degradation of several liquid and solid organic compounds, including polymers, with molecular weights covering a wide range from 600 to 500,000 was studied on TiO_2 thin films on glass under UV illumination. Nearly exact agreement was found between the weight losses of the solid compounds octadecane and stearic acid and the weights of CO_2 produced during photocatalytic degradation. No other gas-phase degradation product was detected for these two compounds other than CO_2, which means that potentially harmful products are not expected to pose a problem. For convenient comparison of degradation rates for various compounds and measurement methods, the values were converted to numbers of moles of carbon reacted per square centimeter per hour. Under appropriate conditions (50°C, relative humidity 10% in air), octadecane was completely decomposed (<400 ng cm^{-2}). In contrast, stearic acid did not decompose completely, even after more than 80 h of UV illumination. This may be due to the formation of a photocatalytically inert reaction product that blocks the TiO_2 surface. The decomposition rates for all of the compounds examined spanned less than two orders of magnitude, suggesting that the photocatalytic reactions involved are rather versatile. © 2000 Published by Elsevier Science B.V.

Keywords: Titanium dioxide; Photocatalyst; Self-cleaning; Reaction intermediates

1. Introduction

Since the first report on photoinduced water splitting by titanium dioxide electrodes was published [1], a variety of different types of photoprocesses have been studied on this material. TiO_2 has been studied extensively as a photocatalyst for organic synthesis [2–6] and for environmental cleanup [7–9]. More recent applications of TiO_2 as a photocatalyst and photoactive material have involved antifouling [10], deodorizing [11], antibacterial [12] and self-cleaning functions [13,14]. Much work has been carried out on the photocatalytic decomposition of relatively small organic compounds, either in gas or liquid phase [15]. However, a much smaller body of work exists for the photodecomposition of higher molecular weight organic compounds. Such compounds are of much practical interest, because they are commonly encountered contaminants on indoor wall surfaces, particularly in kitchens, as well as in other enclosed situations, for example, inside highway tunnels [16].

The reaction mechanisms for solid compounds are expected to have both similar and dissimilar aspects compared to those for gaseous and liquid compounds. For example, one difference expected is that the photodecomposition products for smaller compounds are more likely to escape from the photocatalyst surface as gases than those from solids. Little work has been carried out on the study of mechanisms, although we have recently reported atomic force microscopic (AFM) experiments on Langmuir–Blodgett films of stearic acid adsorbed on rutile single crystals during the course of photocatalytic decomposition [17].

It is well known that gas–solid photocatalytic reactions on TiO_2 are influenced by several different factors, for example, the surface and solid-state properties of the photocatalyst, the type of compound being decomposed, the compound loading, the temperature, and parameters associated with the gas atmosphere, such as the humidity. The influence of such variables has been examined in the present work. The compounds examined have included octadecane, stearic acid, glycerol trioleate, glycerol, paraffin, salad oil, and polyethylene glycol. The experimental methods have

* Corresponding author.

1010-6030/00/$ – see front matter © 2000 Published by Elsevier Science B.V.
PII: S1010-6030(00)00350-6

included gas and liquid chromatography and Fourier transform infrared (FTIR) spectroscopy.

2. Experimental section

2.1. Catalyst preparation

Three types of TiO_2 thin films were used in this work. For type I, TiO_2 thin films were prepared on soda lime glass from tetraisopropoxide in ethyl acetate (10–30%)–isopropanol (5–25%, Nippon Soda Co.) by a dip-coating process. After being dip-coated, the film was calcined at 500°C for 30 min. The thickness of the translucent anatase TiO_2 film was ~0.4 μm. For type II, TiO_2 thin films were prepared by the pyrosol process, in which the atomized mist produced by ultrasonication of the same tetraisopropoxide solution was carried by air flow into an electric muffle furnace at 500°C. For type III, nanocrystalline TiO_2 powder (Ishihara Sangyo Co., Japan) ST-11 (anatase type; particle size, 20 nm; specific surface area, 60 $m^2\,g^{-1}$) was supported on glass substrates by use of an inorganic binder. The apparent area of the TiO_2 thin films was 25 cm^2. They were confirmed to be completely in the anatase form by the presence of the 144, 197, 497, 516, and 614 cm^{-1} Raman peaks. The films were stored in ambient air prior to use.

2.2. Sample preparation

The organic compounds used (see Table 1) were deposited on the TiO_2 photocatalyst surface as follows. Stearic acid was applied as a saturated solution in *n*-hexane onto the TiO_2 film to give a net weight of 44 μg cm^{-2}. Octadecane was first liquefied by heating. The resulting viscous liquid was then spread evenly on the TiO_2 surface to give a net weight of 28 μg cm^{-2}. In the same manner, glycerol trioleate (100 μg cm^{-2}) was spread evenly on the TiO_2 surface. All chemicals (analytical reagent grade) were obtained from Wako Chemical Co. and were used without further purification. A sealed 1 l Pyrex glass vessel was employed as the photoreaction vessel. In a typical photocatalytic experiment, the organic compound coated on the TiO_2 sample was placed on the bottom of the photoreaction vessel and UV light (light from a Hg–Xe lamp was passed through a 365 nm band-pass filter) was used to illuminate the sample through a Pyrex window at the top of the vessel. Typical UV light intensities (controlled by use of sheets of metal gauze) at the sample surface were in the range of 0.1–1.1 mW cm^{-2}. Synthetic air (21% O_2–79% N_2) was used as the usual atmosphere, without humidification; a small amount of water was present initially due to that contained in the TiO_2 film itself. However, even after equilibration for ~1 h in the dark, the relative humidity (RH) was less than 10%. In some cases, the atmosphere was humidied to >90% RH. Unless so specified, the atmosphere used was dry (<10% RH). The photodegradation processes were followed by measuring the CO_2 evolution and changes in sample weight, by gas chromatography (GC) and by use of an electronic balance (Mettler Toledo, 10 μg precision), respectively.

2.3. IR spectra

The photodegradation processes were also examined by use of Fourier-transform infrared (FT-IR, JASCO, FTIR-8900) spectroscopy. However, in this case, TiO_2 films were deposited onto CaF_2 plates. The titanium tetraisopropoxide solution was diluted 1:1 (v/v) with distilled water and an initial coating (~0.05 μm) was applied in order to improve adhesion. The final coating thickness was ~0.4 μm.

2.4. Product analysis

Reaction intermediates were analyzed by GC (Shimadzu GC-8A equipped with a 2.5 m Porapak-Q column for CO_2, a 2.0 m SE-30 column for residual by-products, and flame ionization detector (FID)). N_2 was used as the carrier gas. Due to the lack of response of the FID to CO_2, a methanizer (Shimadzu MTN-1 loaded with reduced Shimadzu shimalite-Ni catalyst), which reduces CO_2 to methane, was

Table 1
Characteristics of samples

Compound name	Compound IUPAC name or synonyms	Stoichiometric formula	Molecular weight	Melting point (°C)
Octadecane	*n*-Octadecane	$C_{18}H_{38}$	254.50	28.28
Stearic acid	*n*-Octadecanoic acid	$C_{18}H_{36}O_2$	284.48	69.3
Glycerol trioleate	9-Octadecenoic acid (*Z*), 1,2,3-propanetriyl ester	$C_{57}H_{104}O_6$	885.45	−5
Glycerol	1,2,3-Propanetriol	$C_3H_8O_3$	92.094	17.8
Liquid paraffin[a]	Mineral oil		247	−12.5 (pour-point)
Salad oil[b]			280	−5 to −10
	cis-9-octadecenoic acid	$C_{18}H_{34}O_2$	282.47	13.4
	9,12-octadecadienoic acid	$C_{18}H_{32}O_2$	280.45	−5
	all-*cis*-9,12,15-octadecatrienoic acid	$C_{18}H_{30}O_2$	278.43	−11.3
	n-hexadecanoic acid	$C_{16}H_{32}O_2$	256.43	62
PEG (MW 600 D)	Poly(ethylene glycol)	$[C_2H_6O_2]_n$	600	15–25
PEG (MW 50 kD)	Poly(ethylene glycol)	$[C_2H_6O_2]_n$	500000	57–65

[a] Including 15–20-carbon hydrocarbons, alkyl naphthalene hydrocarbons.
[b] Including oleic, linoleic, linolenic, and palmitic acids (IUPAC names shown) and stearic acid (already listed above).

attached to the GC system between the column and the detector. The sample gas was collected by a syringe from the vessel. Residual by-products that remained on the TiO_2 surface were extracted with ethanol. In order to improve separation, temperature programmed chromatography was used. A 0.5 μl aliquot of the extracted solution was injected. The temperature of the column (SE-30) was ramped from 100 to 280°C at a rate of 10°C min^{-1}.

3. Results

Fig. 1 shows the extent of reaction as a function of time for the TiO_2-mediated photodegradation of octadecane at 25°C. The reaction started immediately after UV illumination commenced. Only CO_2 was detected by GC in the gas phase. Furthermore, CO_2 was produced from the beginning of the reaction. The weight changes of octadecane and evolved CO_2 concentrations were converted into amounts of carbon (in moles) per unit area (Fig. 1B). Within experimental error, both plots are superimposable. This indicates that the gas-phase product CO_2 is produced stoichiometrically by the solid-phase photoreaction of octadecane.

The initial portions of the curves were linear (Fig. 1A). Octadecane was photooxidized by pseudo-zero-order kinetics during the first 25 h. In a solid-phase reaction, the following condition holds: $[C] = [C_0]$ = constant, and $-\mathrm{d}[C]/\mathrm{d}t = k_1[C_0] = k_0$, where k_1 is the first order rate constant and k_0 is the pseudo-zero-order rate constant (Table 2). The effective concentration of solid reactant is

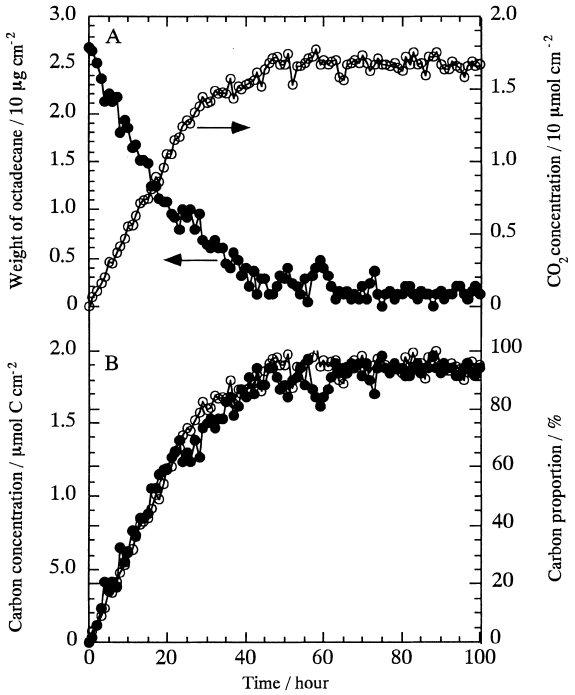

Fig. 1. Plots of (A) weight changes (●) and CO_2 concentration (○) vs. illumination time; and (B) the same data plotted in terms of the number of moles (left axis) and the percentage of the initial amount of carbon (right axis) for the photodecomposition of octadecane, at 25°C. Incident light intensity = 0.8 mW cm^{-2}. Rate constants of weight change and CO_2 production in initial 25 h were 0.70 and 0.74 μg cm^{-2} h^{-1}, respectively.

Table 2
The initial rate constants for the photodecomposition of octadecane, octadecanoic acid, and glycerol trioleate

Samples	Measurements	Film preparation method	Light intensity (mW cm^{-2})	Rate constants		
				μg cm^{-2} h^{-1}	nmol Sample cm^{-2} h^{-1}	nmol C cm^{-2} h^{-1}
Octadecane	Weight change	Dip-coating	0.8	0.70	2.8	50
	Weight change	Dip-coating	1.1	0.84	3.3	59
	CO_2 production	Dip-coating	0.8	0.74	2.9	52
	CH_2	Dip-coating	1.1	–	–	50
	CH_3	Dip-coating	1.1	–	–	6.4
Stearic acid	Weight change	Dip-coating	0.8	0.75	2.7	48
	CO_2 production	Dip-coating	0.8	0.82	2.9	52
Glycerol trioleate	Weight change	Dip-coating	1.1	6.6	7.4	420
	CO_2 production	Dip-coating	1.1	6.6	7.4	420
	CH_2	Dip-coating	1.1	–	–	330
	CH=	Dip-coating	1.1	–	–	72
	Weight change	Pyrosol	1.1	9.6	11	620
Glycerol	Weight change	Pyrosol	1.1	31	340	1000
Liquid paraffin	Weight change	Pyrosol	1.1	7.6	31	540
Salad oil	Weight change	Pyrosol	1.1	6.2	22	390
PEG (MW = 600)	Weight change	Pyrosol	1.1	17	28	280
	Weight change	Binder	1.1	22	37	370
PEG (MW = 500,000)	Weight change	Pyrosol	1.1	12	0.024	190
	Weight change	Binder	1.1	13	0.026	210

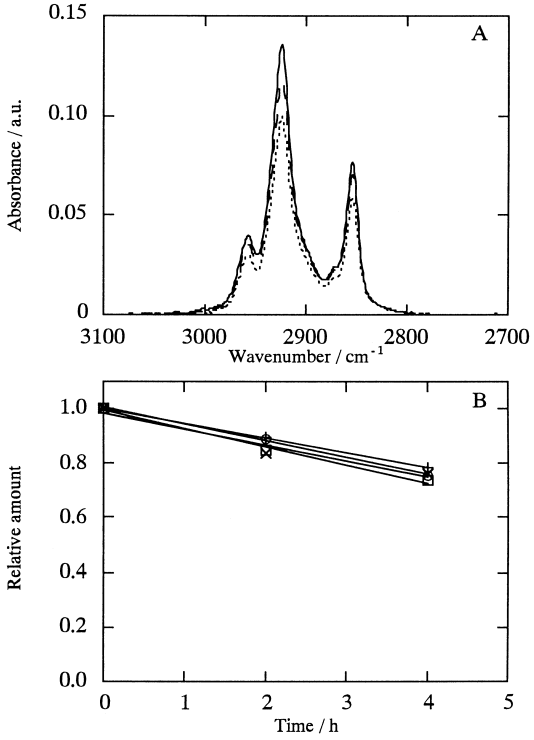

Fig. 2. Plots of (A) IR spectra after 0 h (solid line), 2 h (dashed line), and 4 h (dotted line); (B) weight change (○), absorbance by antisymmetric stretch 2925 cm^{-1} (□) and symmetric stretch 2850 cm^{-1} (+) of CH_2, and antisymmetric stretch 2960 cm^{-1} (×) of CH_3 vs. illumination time for the photodecomposition of octadecane at 25°C. Incident light intensity = 1.1 mW cm^{-2}.

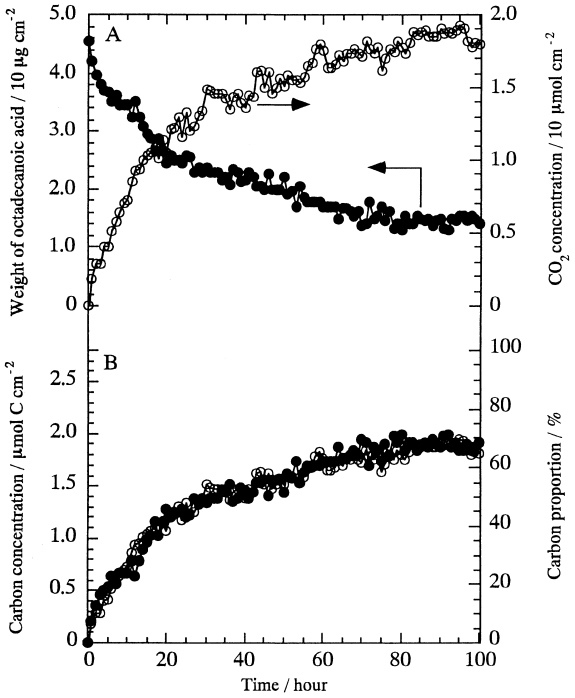

Fig. 3. Plots of (A) weight changes (●) and CO_2 concentration (○) vs. illumination time; and (B) the same data plotted in terms of the number of moles (left axis) and the percentage of the initial amount of carbon (right axis) for the photodecomposition of stearic acid at 25°C. Incident light intensity = 0.8 mW cm^{-2}. Rate constants of weight change and CO_2 production in initial 25 h were 0.75 and 0.82 μg cm^{-2} h^{-1}, respectively.

high and can be approximated by a constant value. The corresponding film thinning rates were ca. 9–11 nm h^{-1}.

IR spectra collected at various times for the TiO_2 film cast on a CaF_2 plate show that the amounts of $–CH_2–$ (estimated from the heights of the 2850 and 2925 cm^{-1} peaks) and $–CH_3$ (estimated from the height of the 2960 cm^{-1} peak) groups decrease similarly in the photodegradation of octadecane (Fig. 2A and B). The photodecomposition of octadecane again appears to follow pseudo-zero-order kinetics, based on the linear plots of absorbance versus time (Fig. 2B). The 2960, 2850 and 2925 cm^{-1} absorbance peaks are assigned to the antisymmetric stretch for the $–CH_3$ group, and the symmetric and antisymmetric stretches for the $–CH_2–$ groups, respectively.

Decomposition rates M (mol cm^{-2} h^{-1}) were calculated on the basis of the numbers of carbon atoms of the $–CH_2–$ and $–CH_3$ types from the IR absorbance changes by use of the following equation: $M = TA$, where T is the total amount of sample (corrected for carbon type) per unit area (mol cm^{-2}), calculated from the initial weight, and A the decomposition rate (h^{-1}) calculated as the slope of the relative amount versus time behavior (Fig. 2B). The values, given in Table 2, are in good agreement with those obtained from the weight changes. The sum of the values for the $–CH_2–$ and $–CH_3$ type carbons ($50 + 6.4 = 56.4$ nmol C cm^{-2} h^{-1}) is close to the value for all carbons (59 nmol C cm^{-2} h^{-1}), obtained from the weight change measurements. In addition, the rates normalized by the relative numbers of carbons of both types, i.e. assuming that the whole molecule was composed of the same type of group, were nearly the same, 56 and 58 nmol C cm^{-2} h^{-1}, respectively for $–CH_2–$ and $–CH_3$ groups. This is reflected by the approximately equal slopes in Fig. 2B. Peaks for other types of functional groups (e.g. carbonyl, aldehyde, and carboxyl) did not appear in the spectra during the photodecomposition of ocatadecane. These results show that the amounts of intermediates were relatively small.

Typical extent of reaction versus time plots for the photooxidative degradation of stearic acid and glycerol trioleate are presented in Fig. 3A and B and Fig. 4A and B, respectively. Both were also photooxidized by pseudo-zero-order kinetics in the initial period (up to 20 h). Likewise, no gaseous intermediates were detected. The weight change versus time behavior for octadecane and stearic acid yielded similar rates, i.e. 0.70 (50) and 0.75 μg cm^{-2} h^{-1} (48 nmol C cm^{-2} h^{-1}), respectively. The initial CO_2 production rate for stearic acid, 52 nmol C cm^{-2} h^{-1}, was also in good agreement. The corresponding film thinning rates were ca. 8–9 nm h^{-1}. The decomposition rate for glycerol trioleate on a per carbon basis (420 nmol C cm^{-2} h^{-1}) was much higher (ca. 8×) than those for octadecane or stearic acid.

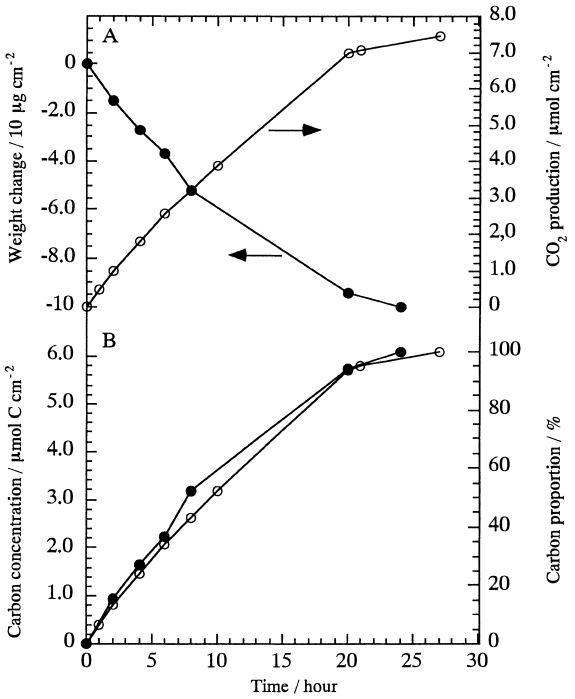

Fig. 4. Plots of (A) weight changes (●) and produced CO_2 concentration (○) vs. illumination time; and (B) the same data plotted in terms of the number of moles (left axis) and the percentage of the initial amount of carbon (right axis) for the photodecomposition of glycerol trioleate at 25°C. Incident light intensity = 1.1 mW cm^{-2}. Rate constants of weight change and CO_2 production in initial 20 h were 6.6 and 6.6 μg cm^{-2} h^{-1}, respectively.

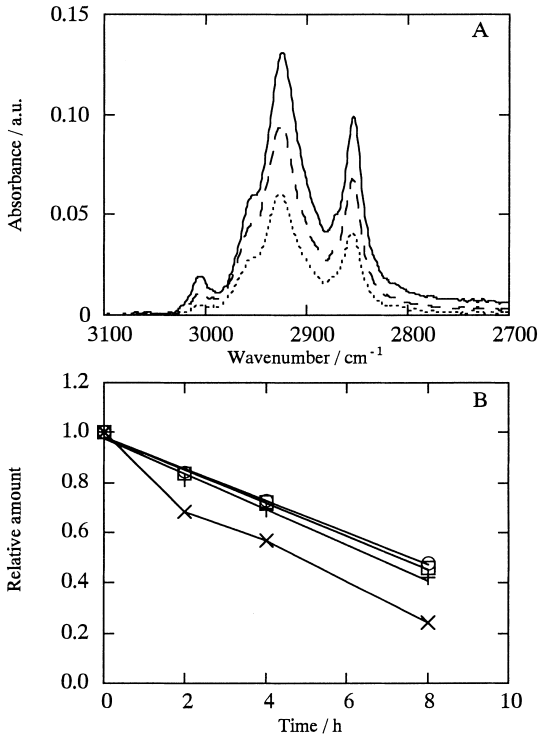

Fig. 5. Plots of (A) IR spectra after 0 h (solid line), 2 h (dashed line), and 4 h (dotted line); (B) weight change (○), absorbance by antisymmetric stretch 2925 cm^{-1} (□) and symmetric stretch 2850 cm^{-1} (+) of CH_2, and stretch 3020 cm^{-1} (×) of =CH– vs. illumination time for the photodecomposition of glycerol trioleate at 25°C. TiO_2 thin films prepared by the dip-coating method. Incident light intensity = 1.1 mW cm^{-2}.

Decomposition rates were also determined for glycerol trioleate from the time dependence of the IR spectra for the –CH_2– and =CH– groups (Fig. 5A and B), and the rate for the decomposition of –CH_2– groups was also relatively high (330 nmol C cm^{-2} h^{-1}). The sum of the rates for –CH_2– and =CH– groups (330 + 36 = 366 nmol C cm^{-2} h^{-1}) was somewhat less than the value for all types of carbon obtained from weight loss (420 nmol C cm^{-2} h^{-1}). Interestingly, the respective rates, after being normalized to the relative amounts of the two types of carbons, i.e. the =CH– (16 mol% h^{-1}) and –CH_2– groups (9.5 mol% h^{-1}), show that the =CH– group is much easier to photodecompose than the –CH_2– group. This is also reflected in the slopes of the plots in Fig. 5B.

The apparent quantum yields were calculated by use of the following expression: $\phi = M/P$ where M is the number of decomposed molecules per unit area per unit time (cm^{-2} h^{-1}), and P is the number of incident photons per unit area per unit time (cm^{-2} h^{-1}). The apparent quantum yields for octadecane and stearic acid were almost identical, 0.032 and 0.031, respectively, and that for glycerol trioleate was 0.063.

The decomposition behavior of various types of oils are compared in Fig. 6. The photodecomposition rate for glycerol (1010 nmol C cm^{-2} h^{-1}, 31 μg cm^{-2} h^{-1}) was significantly faster than those for the other oils: glycerol trioleate (620 nmol C cm^{-2} h^{-1}, 9.6 μg cm^{-2} h^{-1}), liquid paraffin (7.6 μg cm^{-2} h^{-1}), and salad oil (6.2 μg cm^{-2} h^{-1}) which consisted of oleic acid, linoleic acid and linolenic acid as principal components.

One of the possible factors related to these differences in decomposition rates could be differences in the melting point (mp). In order to test this hypothesis, various compounds

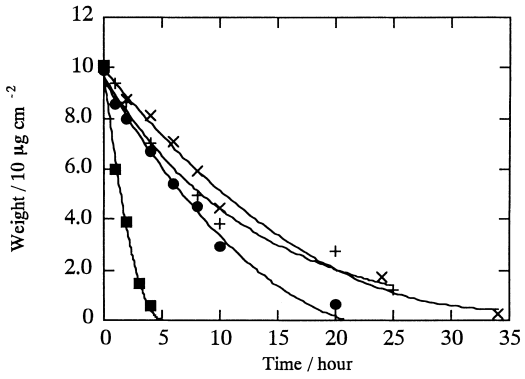

Fig. 6. Plots of weight changes vs. illumination time for the photodecomposition of glycerol trioleate (●) and glycerol (■) liquid paraffin (+) salad oil (×) at 25°C. TiO_2 thin films were prepared by the pyrosol method. Incident light intensity = 1.1 mW cm^{-2}. Rate constants of weight change of glycerol trioleate, glycerol, liquid paraffin, and salad oil in initial 2 h were 9.6, 31, 7.6 and 6.2 μg cm^{-2} h^{-1}, respectively.

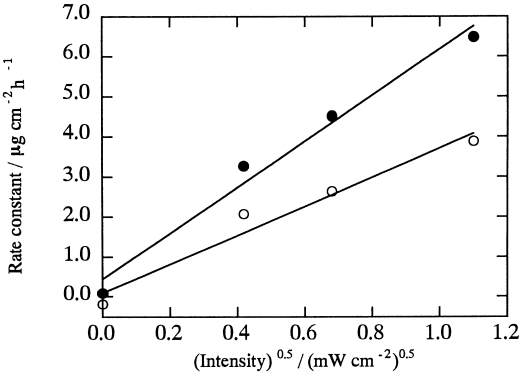

Fig. 7. Plots of rate constant vs. the square root of light intensity for the photodecomposition of PEG (MW 600) at 25°C. TiO_2 thin films were prepared by the pyrosol (●) and binder (○) techniques.

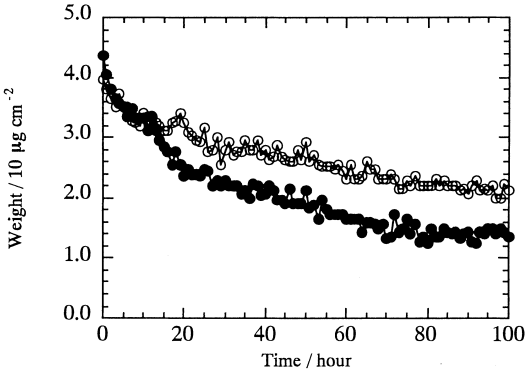

Fig. 9. Plots of weight changes vs. illumination time for the photodecomposition of stearic acid at 25°C in a dry atmosphere (<10% RH) (●) and a humid atmosphere (>90% RH) (○). Rate constants of weight change under low and high humidity conditions in initial 25 h were 0.75 and 0.32 μg cm^{-2} h^{-1}, respectively.

were used to examine the effect of mp (Table 2). The mp of octadecane is larger than that of glycerol trioleate, and the rate constant of the former is lower than that of the latter. On the other hand, the mp of stearic acid is different from that of octadecane, but both have nearly the same rate constant. The molecular weight (MW) of stearic acid is nearly equal to that of octadecane. The lower the mp, the larger the rate constants are in liquid paraffin, salad oil, PEG (MW = 600) and PEG (MW = 500,000) except glycerol. The MW of glycerol is relatively small compared with the other compounds.

Under conditions of moderate to high light intensity, the photocatalytic oxidation rate is often found to depend on the square root of light intensity [18]. This rule also appears to hold true for PEG (MW = 600) (Fig. 7). This result indicates that the rate is limited by recombination under these particular conditions. The effect of light intensity on other compounds has not been examined thus far.

On varying the initial weight of octadecane on the titanium dioxide thin film, the photooxidation rate was constant over the first 25 h for two different loadings (Fig. 8). Beyond 25 h the photodegradation rates approached constant values that depended upon the initial weight. The photodegradation of PEG (MW = 600) showed a similar tendency.

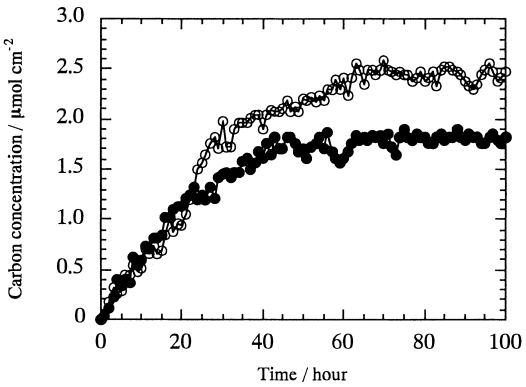

Fig. 8. Plots of produced CO_2 concentrations vs. illumination time for the photodecomposition of octadecane at 25°C. Initial weight = 0.65 mg (●) and 0.90 mg (○). Incident light intensity = 0.8 mW cm^{-2}.

The CO_2 production rate in the photodecomposition of stearic acid is known to depend on the light intensity and on the O_2 and H_2O partial pressures [19] [1]. In the present work, the effect of high relative humidity (>90% RH) was compared to that of the normal dry atmosphere (<10% RH). The photooxidation rate (20 nmol C cm^{-2} h^{-1}) obtained under high humidity conditions was lower than that (48 nmol C cm^{-2} h^{-1}) obtained under low humidity conditions (Fig. 9).

Octadecane completely photodecomposed (<400 ng cm^{-2}), as seen in Fig. 1A. However, stearic acid did not decompose completely, even after more than 80 h of UV illumination (Fig. 3A). As seen in Fig. 9, the amount of residual sample and intermediates remaining under high humidity conditions (54% of the initial weight) was greater than that remaining under low humidity conditions (31% of the initial weight).

In general, as the reaction temperature is raised, the photocatalytic activity is expected to increase. Indeed, in the present work, the decomposition rate for stearic acid at 50°C (86 nmol C cm^{-2} h^{-1}) was larger than that at 25°C (48 nmol C cm^{-2} h^{-1}). Similarly, the amounts of residual sample and reaction products obtained at 50°C (19% of the initial weight) were less than those obtained at 25°C (31% of the initial weight) (Fig. 10). We also note that these reaction products are rather inert: after having formed at 25°C, they do not undergo significant reaction even after the temperature is raised to 50°C.

[1] In the present work, the stearic acid film thickness was 5200 Å, whereas it was 2000 Å in Ref. [19]. In the present work, the maximum CO_2 generation rate corresponding to the consumption of stearic acid was 51 nmol C cm^{-1} h^{-1} under 0.8 mW cm^{-2} illumination, and this increased to 86 nmol C cm^{-1} h^{-1} under 2.4 mW cm^{-2} illumination in a dry atmosphere. The corresponding values taken from Fig. 2 in Ref. [19] were 29 and 47 nmol C cm^{-1} h^{-1}, respectively, for high humidity conditions. These differences are relatively slight, well within the variations expected for different films.

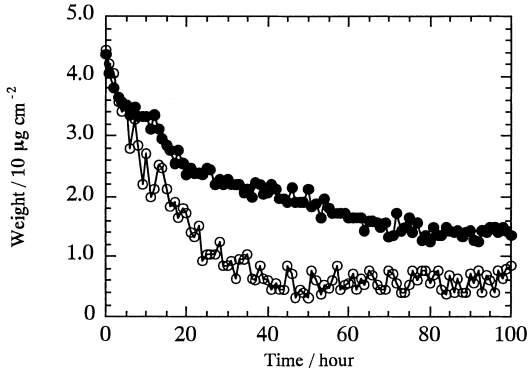

Fig. 10. Plots of weight changes vs. illumination time for the photodecomposition of stearic acid at 25°C (●) and 50°C (○). Incident light intensity = 0.8 mW cm^{-2}. Rate constants of weight change at 25 and 50°C in initial 25 h were 0.75 and 1.4 μg cm^{-2} h^{-1}, respectively.

The residues remaining after stearic acid was illuminated with UV light for 5 h and, in a separate experiment, for 20 h, on TiO_2 surfaces were analyzed by use of GC. Most of the residue was unreacted stearic acid (99.4 and 95.4 mol% for 5 and 20 h, respectively). A number of minor products were also detected. The two largest product peaks exhibited the same retention times as heptadecanoic acid and hexadecanoic acid according to results obtained under the same conditions with the actual compounds. A few broad peaks were observed at retention times greater than those for ordinary, low-molecular-weight compounds, indicating that these were due to polymerized products. GC–mass spectrometric measurements were attempted, but it was difficult to identify these products positively due to the small amounts (1.90% based on the initial number of moles of carbon).

After 5 h of illumination, the total amount of solid product, i.e. other than stearic acid itself, was 0.45% based on the initial number of moles of carbon (Table 3). When the sample was illuminated for 20 h, almost the same product peaks were observed with GC, and the total amount was 1.90% based on the initial number of moles of carbon. Thus, it appears that the amounts of solid products existing during the photodegradation of stearic acid reaches an approximate steady state after 5 h of illumination.

The moles of carbon corresponding to evolved CO_2 obtained after 5 and 20 h were 0.51 and 1.3 μmol C cm^{-2}, respectively. These values are in good agreement with the values obtained from weight loss from the film after 5 and 20 h, 0.53 and 1.3 μmol C cm^{-2}, respectively. This result indicates that there were negligible amounts of gas-phase products other than CO_2.

Table 3
Distribution of carbon (starting material, carbon dioxide and solid products) in the photodecomposition of stearic acid for two illumination times (5 and 20 h) at 25°C in a dry atmosphere (<10% RH)[a]

Times (h)	Carbon dioxide (%)	Carbonaceous residues	
		Octadecanoic acid (%)	Intermediates (%)
5	18.8	80.8	0.48
20	46.4	51.1	2.43

[a] Incident light intensity = 0.8 mW cm^{-2}.

4. Discussion

The results for the photocatalytic decomposition of octadecane, stearic acid and glycerol trioleate show that this process proceeds at significant rates (from ca. 50 to ca. 1000 nmol C cm^{-2} h^{-1}), with the evolution of CO_2 as the only detectable gas-phase product (detection limit of ∼3.5 nmol cm^{-2} h^{-1} for acetone, ∼1.2 nmol cm^{-2} h^{-1} for formaldehyde, etc.) at moderate light intensities (0.8–1.1 μW cm^{-2}). This is an important result, because it shows that photocatalysis can be used to decompose organic films without the generation of toxic gas-phase products, as also previously reported by others [19].

Furthermore, in the case of octadecane and glycerol trioleate, a semi-liquid and a liquid, respectively, at room temperature, the reaction goes to completion after periods of 25–50 h. This is also an important result, because it shows that organic films of this type, e.g. oils, can be completely decomposed over reasonable time periods.

In contrast, however, in the case of stearic acid, the photocatalytic decomposition did not go to completion but essentially came to a halt after ∼69% of the compound had been decomposed at close to 100 h, when the original film thickness was 520 nm. This type of effect has also been observed by Sitkiewitz and Heller for the decomposition of benzene under dry conditions [19]. These workers ascribe the effect to the formation of polymeric products that block the TiO_2 surface. In the absence of water, the photocatalytic reactions are presumably forced into pathways in which organic radicals can couple. A blocking reaction was not observed with stearic acid in that work, because the measurements were confined to about 4 h, rather than up to 100 h, as in the present work. With benzene, the effect is more significant, and there it was observable during relatively short illumination times. They found that a brown material formed on the TiO_2 film in the absence of water, and this material was difficult to dissolve in most organic solvents. This result is consistent with ours, in which we found products with relatively long GC retention times.

From the present results, it is clear that polymers in general are far from inert towards photocatalytic decomposition. Therefore, assuming that oligomeric products of some type are responsible for deactivating the TiO_2 film, there must be other factors involved. We propose that a small fraction of the products that can form under dry conditions must be able to react with photogenerated holes in ways that do not lead to decomposition, e.g. because they form relatively stable radicals. Certain types of organic radicals are easily formed, e.g. highly branched hydrocarbons, i.e. with secondary or tertiary hydrogens, and those with carbonyl groups [20].

Both of these types could conceivably be produced during photocatalytic reactions. Products with carbonyl groups are already shown in Scheme 3. Chain branching could occur in cases of radical coupling. This is an issue that deserves further investigation because of its importance in maintaining the activity of photocatalysts.

Another possible explanation is that parts of the stearic acid film may lose intimate physical contact with the TiO_2 surface and thus may not be exposed to high enough concentrations of active oxygen radicals. This explanation is not as likely, however, because our group has also found that photocatalytic reactions can still take place at distances up to ca. 100 μm away from the surface of an illuminated TiO_2 film, although the reaction rates decrease significantly with distance [21]. The only evidence for this idea in the present work is indirect: a semi-solid (octadecane) and a liquid (glycerol trioleate) were able to undergo complete decomposition, suggesting that they remain in contact with the surface more effectively than does a solid film.

The present results for the photocatalytic decomposition of stearic acid also show that the films can be decomposed effectively in a dry atmosphere, suggesting that the water that is generated during the decomposition can be effectively used. This result is the only one that appears to be inconsistent with those of Sitkiewitz and Heller [19]. In fact, in comparing their decomposition rates (specifically, CO_2 generation rates) under high humidity conditions at $0.8\,mW\,cm^{-2}$ ($29\,nmol\,C\,cm^{-2}\,h^{-1}$) with our result at the same light intensity ($23\,nmol\,C\,cm^{-2}\,h^{-1}$), there is remarkable agreement. However, under dry conditions, our rate constant (ca. $50\,nmol\,C\,cm^{-2}\,h^{-1}$) was about an order of magnitude greater than theirs ($<3.6\,nmol\,C\,cm^{-2}\,h^{-1}$).

This discrepancy is explainable, but the explanation is speculative at this point. There are most likely differences in the TiO_2 morphology that would either allow or not allow water generated during the photocatalytic process to continue to participate in further reaction. However, the film characteristics in the present work (ca. 400 nm thick; 500°C, 30 min. calcination) are very similar to those used in the other work (ca. 300 nm thick; 550°C, 30 min. calcination). Even so, there can be differences in morphology caused by subtle differences in the preparation procedures.

The other aspect that needs to be explained is why excess humidity was detrimental in the present work and beneficial in the other work. We propose specifically that the film pore structures might be different. In the present work, the pores may be smaller, which would both help to retain water generated by the photocatalytic reaction but would also cause the film to become flooded in the presence of excess water. These types of differences should be examined more carefully in future work.

It is clear that there is no single characteristic of the organic compound that controls its photocatalytic decomposition rate. For example, the fact that a compound is a liquid or solid at room temperature appears not to be all-important, although there is a semblance of a correlation between rate and melting point (Fig. 11). As already discussed, this trend is relatively slight and might be more of a controlling factor in the long-term decomposition than in the short-term decomposition (viz., octadecane and stearic acid).

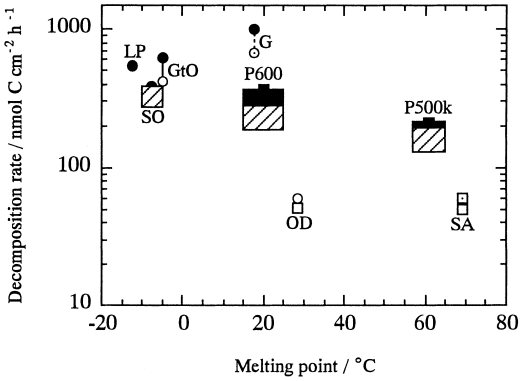

Fig. 11. Plots of photodecomposition rate vs. melting point for stearic and glycerol trioleate by use of TiO_2 thin films prepared by the dip-coating method under $1.1\,mW\,cm^{-2}$ illumination (○); for the photodecomposition of octadecane and stearic acid by use of TiO_2 thin films prepared by the dip-coating method under $0.8\,mW\,cm^{-2}$ illumination (□); for the photodecomposition of glycerol, glycerol trioleate, liquid paraffin, salad oil, and PEG (MW = 600, and 500,000) by use of TiO_2 thin films prepared by the pyrosol method under $1.1\,mW\,cm^{-2}$ illumination (●); for the photodecomposition of PEG (MW = 600, and 500,000) by use of TiO_2 thin films prepared by the binder method under $1.1\,mW\,cm^{-2}$ illumination (■). Abbreviations: G: glycerol; GtO: glycerol trioleate; LP: liquid paraffin; OD: octadecane; SA: stearic acid; P600 = PEG (MW = 600), P500k = PEG (MW = 500,000); SO: salad oil. An open square containing a dot is shown for the decomposition rate expected for SA at $1.1\,mW\,cm^{-2}$. Hatched areas are shown for the rates expected for P600, P500k and SO (open circle containing a dot for G) for decomposition on a dip-coated TiO_2 film, based on the comparison for GtO.

One additional way to examine the effect of the melting point is by varying the temperature. This was done for stearic acid, although both temperatures were below the mp. The major difference was in the degree of completion of the decomposition at long times. At 50°C, even though the compound was still below the mp, (69°C), the reaction proceeded to a significantly greater extent, so that ca. 81% of the original starting material was decomposed, as opposed to 69% at room temperature.

One factor that controls the melting point, other than molecular weight, is the degree of hydrogen bonding. This factor helps to raise the melting points of stearic acid and glycerol. However, this factor alone does not appear to affect the decomposition rates. Another factor is the molecular weight itself, but again, this is not by itself a strong controlling factor. If we compare two different molecular weight PEG samples, we see only a small difference in rates.

Yet another factor that can be considered is the wettability. This factor is quite complex, because our group has already shown that TiO_2 rutile surfaces can exhibit both hydrophilicity and oleophilicity, both photoinduced [22]. In any case, this factor may be involved in the greater than expected photodecomposition rates for glycerol and glycerol trioleate.

The similarity of the results for the photocatalytic decomposition of these three compounds, octadecane, stearic acid and glycerol trioleate suggests that the mechanisms may also be similar. The fact that different types of compounds can react in a similar fashion also suggests that the mechanisms are of a general type.

By illuminating TiO_2 surfaces with >3.2 eV light, electrons are excited from the valence band to the conduction band, forming electron-hole pairs. The surviving electrons can react with O_2 to produce superoxide ions ($O_2^{\bullet -}$) [23–27]. Hydroxyl radicals can be produced by the reaction of water with holes [28,29].

Thenceforth, the generated $^{\bullet}OH$ and $O_2^{\bullet -}$ radicals may participate in schemes that have been proposed previously (Scheme 1) [19]. These types of reactions are known to be important in the decomposition of various types of organic compounds, i.e. alkanes, alcohols, ketones and carboxylic acids [9].

However, this type of scheme cannot explain the presence of the C_{16} and C_{17} acids, which were detected in the decomposition of stearic acid. In order to explain their presence, a pathway involving carbene intermediates may be important, as proposed by Schwitzgebel et al. (Scheme 2) [30].

The present results strongly suggest that long-chain organic compounds and even polymers may react so that the chains are broken. In order for this to happen, one of the possibilities is that one of the carbons in the hydrocarbon chain must react so that a carbonyl group is introduced (Scheme 3) [15]. Thenceforth, the chain is broken, and two aldehydes are produced, which are thought to decompose quickly.

The overall results show that a variety of long-chain liquid and semi-solid organic compounds can be photocatalytically decomposed to completion with the absence of toxic gas-phase products. The decomposition rates cover less than two orders of magnitude (ca. 50–1000 nmol C cm^{-2} h^{-1}), again supporting the idea that the mechanisms are of a general type. Even considering the solids, stearic acid and PEG (500,000), the initial decomposition rates are only slightly lower than those for the liquids.

$$RCH_2COOH + h^+ (\bullet OH) \rightarrow RCH_2\bullet + CO_2 + H^+ (H_2O)$$

$$RCH_2\bullet + O_2 \rightarrow RCH_2OO\bullet$$

$$RCH_2OO\bullet + \bullet OOH \rightarrow RCH_2OOOOH$$

$$RCH_2OOOOH \rightarrow RCHO + O_2 + H_2O$$

Scheme 1.

$$CH_3(CH_2)_6COOH + h^+ \rightarrow CH_3(CH_2)_6\bullet + CO_2 + H^+$$

$$CH_3(CH_2)_6\bullet \rightarrow CH_3(CH_2)_5CH + H^+ + e^-_{CB}$$

$$CH_3(CH_2)_5CH + H_2O \rightarrow CH_3(CH_2)_5CH_2OH$$

Scheme 2.

$$RCH(OOOOH)R' \rightarrow RCOR' + O_2 + H_2O$$

$$RCH_2COCH(OOOOH)R' \rightarrow RCHO + R'CHO + CO_2 + H_2O$$

Scheme 3.

5. Conclusions

The most important conclusion from the present work is that films of both a liquid (glycerol trioleate) and a semi-solid (octadecane) can be decomposed on TiO_2 surfaces completely to CO_2. This is important, because it shows that the TiO_2 surface has the ability to self-regenerate. However, for stearic acid, the decomposition came to a halt before completion. We have proposed that this is due to the formation of a small amount of product that is resistant to decomposition, although direct evidence is lacking. This issue requires further study. The present results for stearic acid are roughly consistent with those of Sitkiewitz and Heller [19], with similar decomposition rates. However, in the present work, the reactions were carried out for much longer periods of time (100 versus 4 h), so that the phenomenon of the reaction coming to a halt became apparent. An interesting difference was also observed from that work in terms of the effect of humidity, with high values being detrimental in the present work and beneficial in the previous work. This we propose to involve differences in film morphology, specifically, pore structure; this also deserves further study.

No single characteristic of the compounds examined in this work was recognized as crucial in controlling the photodecomposition rates. However, these rates spanned less than two orders of magnitude, a fact that shows that the photocatalytic reactions are relatively versatile. Reaction mechanisms of the types previously proposed [15] can help to explain such versatility.

References

[1] A. Fujishima, K. Honda, Nature 238 (1972) 37.
[2] M. Fujihira, Y. Satoh, T. Osa, Nature 293 (1981) 206.
[3] B. Kraeutler, A.J. Bard, J. Am. Chem. Soc. 99 (1977) 7729.
[4] D.F. Ollis, Environ. Sci. Technol. 19 (1985) 480.
[5] K. Hashimoto, T. Kawai, T. Sakata, J. Phys. Chem. 88 (1984) 4083.
[6] T. Sakata, T. Kawai, K. Hashimoto, J. Phys. Chem. 88 (1984) 2344.
[7] Y. Nosaka, K. Koenuma, K. Ushida, A. Kira, Langmuir 12 (1996) 736.
[8] X. Fu, W.A. Zeltner, M.A. Anderson, Appl. Catal. B Environ. 6 (1995) 209.
[9] A. Heller, Acc. Chem. Res. 28 (1995) 503.
[10] Y. Paz, Z. Luo, L. Rabenberg, A. Heller, J. Mater. Res. 10 (1995) 2842.
[11] I. Sopyan, M. Watanabe, S. Murasawa, K. Hashimoto, A. Fujishima, J. Electroanal. Chem. 415 (1996) 183.
[12] Y. Kikuchi, K. Sunada, T. Iyoda, K. Hashimoto, A. Fujishima, J. Photochem. Photobiol. A: Chem. 106 (1997) 51.

[13] S. Fukayama, K. Kawamura, T. Saito, T. Iyoda, K. Hashimoto, A. Fujishima, in: Proceedings of the Extended Abstracts of the 187th Meeting of the Electrochemical Society, The Electrochemical Society, Pennington, NJ, USA, 1995.
[14] N. Negishi, T. Iyoda, K. Hashimoto, A. Fujishima, Chem. Lett. 1995 (1995) 841.
[15] J. Schwitzgebel, J.G. Ekerdt, H. Gerischer, A. Heller, J. Phys. Chem. 99 (1995) 5633.
[16] A. Fujishima, in: Abstracts of the Symposium on TiO_2 Photocatalytic Purification and Treatment of Water and Air, Cincinnati, Ohio, USA, 1996.
[17] P. Sawunyama, L. Jiang, A. Fujishima, K. Hashimoto, J. Phys. Chem. B 101 (1997) 11000.
[18] T.A. Egerton, C.J. King, J. Oil Col. Chem. Assoc. 62 (1979) 386.
[19] S. Sitkiewitz, A. Heller, New J. Chem. 20 (1996) 233.
[20] F.A. Carey, R.J. Sundberg, Advanced Organic Chemistry, 3rd Edition, Part A: Structure and Mechanisms, Plenum Press, New York, 1990 (Chapter 12).
[21] T. Tatsuma, S. Tachibana, T. Miwa, D.A. Tryk, A. Fujishima, J. Phys. Chem. B 103 (1999) 8033.
[22] R. Wang, K. Hashimoto, A. Fujishima, M. Chikuni, E. Kojima, A. Kitamura, M. Shimohigoshi, T. Watanabe, Adv. Mater. 10 (1998) 135.
[23] C.D. Jaeger, A.J. Bard, J. Phys. Chem. 83 (1979) 3146.
[24] S. Fukuzawa, K.M. Sancier, T. Kwan, J. Catal. 11 (1968) 364.
[25] C. Naccache, P. Meriaudeau, M. Che, Trans. Faraday Soc. 67 (1971) 506.
[26] P.C. Gravelle, F. Juillet, P. Meriaudeau, S.J. Teichner, Discuss. Faraday Soc. 52 (1971) 140.
[27] K. Ishibashi, Y. Nosaka, K. Hashimoto, A. Fujishima, J. Phys. Chem. B 102 (1998) 2118.
[28] H.G. Voltz, G. Kampf, H.G. Fitzky, Farbe u. Lack 78 (1972) 1037.
[29] J.R. Harbour, J. Tromp, M.L. Hair, Can. J. Chem. 63 (1985) 204.
[30] J. Schwitzgebel, J.G. Ekerdt, F. Sunada, S. Lindquist, A. Heller, J Phys. Chem. B 101 (1997) 2621.